Influence of Andreev reflection on current-voltage characteristics of superconductor/ferromagnet/superconductor metallic weak links

Z. Popović,[1] L. Dobrosavljević-Grujić,[2] and R. Zikic[2,*]
[1]*Department of Physics, University of Belgrade, P.O. Box 368, 11001 Belgrade, Serbia*
[2]*Institute of Physics, University of Belgrade, Pregrevica 118, 11080 Belgrade, Serbia*
(Received 13 February 2012; published 11 May 2012)

We develop a quantitative theory describing the behavior of current-voltage characteristics (CVCs) in superconductor (S)/ferromagnet (F)/superconductor (SFS) weak links with transparent S/F interfaces. The approach of Kümmel, Gunsenheimer, and Nikolsky [Phys. Rev. B **42**, 3992 (1990)], developed for S/normal metal (N)/S junctions with an N barrier and based on the solution of time-dependent Bogoliubov–de Gennes equations combined with the time-relaxation model, is generalized to the SFS case. CVCs are calculated as a function of the barrier material parameters: the exchange energy h, the barrier thickness d, and the mean free path l. CVC peculiarities, such as a steep rise in the current and negative differential conductance at a low voltage, as well as the h-dependent position of the peaks, are obtained for a weak exchange energy h lower than or comparable to the superconducting energy gap $\Delta = \Delta(T)$. They are interpreted to be induced by multiple Andreev reflections, modified in the presence of h in ferromagnets.

DOI: 10.1103/PhysRevB.85.174510 PACS number(s): 74.45.+c, 74.50.+r

I. INTRODUCTION

In recent years, the investigation of metallic weak links has been the subject of many studies. In these structures, consisting of two superconductors (Ss) connected by a normal metal (N) or a ferromagnet (F), SNS or SFS, several static and dynamic properties have been investigated. Among the static ones, the Josephson effect and the proximity effect have been studied experimentally and theoretically, in both SNS and SFS structures.[1–3] The origin of the supercurrent in SNS junctions derives from the existence of Andreev bound states in the N.[4–10] The dynamic properties, which can be revealed by studying the current-voltage characteristics (CVCs) of the junctions, are also closely related to the Andreev scattering.[11] The resistively shunted junction model, commonly used for the description of CVCs, is too simple in comparison with the microscopic theory of Kümmel, Gunsenheimer, and Nikolsky (KGN),[11] which provides several characteristic features of CVCs in the SNS case, such as the "foot" at low voltages, negative differential conductivity, and subharmonic gap structures, in concordance with experiments.[12] A simplified version of this theory, given by Gokhfeld,[13] is used for comparison with experiments on microbridges.[14] A self-consistent method based on the Keldysh formalism for investigation of nonstationary and nonequilibrium balistic charge transport through clean SNS microbridges was developed by Gunsenheimer and Zaikin.[15]

Mesoscopic structures containing S and ferromagnetic elements present an additional point of interest, offering the possibility of studying the competition between the Andreev reflection (AR) and the spin polarization in F parts of such SFS systems.[16] Their static properties have been studied in the case of weakly ferromagnetic alloy barriers, starting with the key experiments done by Ryazanov *et al.*,[17] Kontos *et al.*,[18] Blum *et al.*,[19] Sellier *et al.*,[20] and others, whereas experiments with thin, strongly ferromagnetic metal barriers were performed by Robinson *et al.*[21] and by Bannykh *et al.*[22]

Both static and dynamic properties of SF hybrid structures were investigated experimentally by Pfeiffer *et al.*,[23] Born *et al.*,[24] Krasnov *et al.*,[25] Weides *et al.*,[26] and others. More references for recent experimental and theoretical investigations of both SFS weak links and SIFS (containing an insulator layer; I) tunnel junctions are given by Vasenko *et al.*,[27] who present a theory of CVCs in diffusive SIFS junctions. As for SFS mesoscopic structures, until recently, their dynamic properties have been theoretically investigated only in the case of magnetic point contacts.[16,28] Another recent study deals with the calculation of CVCs in diffusive SFS plane junctions, using the quasiclassical theory of superconductivity.[29]

In the present article, we generalize the approach of KGN[11] to calculate CVCs of dissipative current in SFS weak links. We solve the time-dependent Bogoliubov–de Gennes equations[30] (BdGEs) for Andreev reflected quasiparticles in the presence of the exchange energy in a ferromagnetic barrier. In Fs, we use the Stoner model, and in Ss, the BCS model of superconductivity. CVCs are calculated as a function of the value of the exchange energy in the barrier, barrier thickness, temperature, and mean free path. The S/F interfaces are assumed to be transparent, to achieve a high efficiency of the AR.[31]

In Sec. II, we discuss the model describing the quasiparticle dynamics resulting from the interplay between the energy gain from the electric field and the multiple ARs at S/F interfaces. Generalizing the KGN theory[11] for the SFS case, the time-averaged current density carried by quasiparticle wave packets is calculated in Sec. III using our previous experience in calculating the density of states (DOS) in a ferromagnetic barrier.[32] Results and discussion are presented in Sec. IV, and the conclusions in Sec. V. Some details of the calculations are presented in the Appendix.

II. MODEL AND FORMALISM

We consider a voltage-biased plane SFS junction with a constant electric field in the F layer (which is in the negative

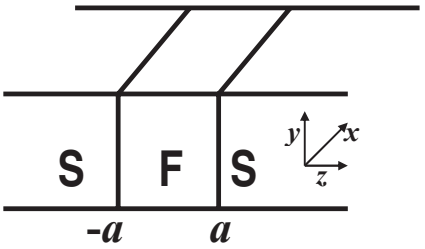

FIG. 1. Scheme of the considered SFS junction.

z direction perpendicular to the S/F interfaces) and negligible field penetration into the superconducting banks. The F layer has a thickness $d = 2a$ of the order of superconducting zero-temperature coherence length ξ_0, while the thickness of the superconducting bank is D, assuming $D \gg 2a$, and cross-section area $L_x L_y$ (Fig. 1). Interfaces between layers are fully transparent. Ss are described in the framework of the standard BCS formalism, neglecting suppression of the pair potential. Although this is a good approximation for thick barriers only, we expect qualitatively the same results for shorter barriers, since the basic physics is in the multiple AR, which is still present.[11] For F we use the Stoner model with an exchange energy shift $2h$ between the spin sub-bands. We work with a weak exchange energy in the F, of the order of the superconducting order parameter, $h \sim \Delta$.

To treat the quasiparticle motion we use the time-dependent BdGEs combined with the relaxation-time model for charge transport under the influence of an electric field and inelastic scattering. In this model, the quasiparticle is freely accelerated by the electric field until time t with probability e^{-t/T_S}, where T_S is the average scattering time. The observable current density (see Sec. III) is proportional to the sum of time averages of all electron and hole momentum densities, where one has to take into account the rate $1/t_c$ at which the quasiparticles start their motion,[11] where

$$t_c = \begin{cases} 2a/v_z, & 2a/v_z < T_S, \\ T_S, & \text{otherwise}, \end{cases} \tag{2.1}$$

and the mean free path l for scattering of the electrons at velocity v_z is $l = v_z T_S$.

Electron-like and hole-like quasiparticles with energy E and spin projection $\sigma = \uparrow,\downarrow$ are described by the time-dependent[30,33] BdGEs, which are

$$\begin{aligned} i\hbar\frac{\partial}{\partial t}u_\sigma(\mathbf{r},t) &= \left[\frac{1}{2m}\left[\mathbf{p}+\frac{e}{c}\mathbf{A}\right]^2 - \mu - \rho_\sigma h\right]u_\sigma(\mathbf{r},t) \\ &\quad + \Delta\Theta(|z|-a)v_\sigma(\mathbf{r},t), \\ i\hbar\frac{\partial}{\partial t}v_\sigma(\mathbf{r},t) &= -\left[\frac{1}{2m}\left[\mathbf{p}-\frac{e}{c}\mathbf{A}\right]^2 - \mu - \rho_\sigma h\right]v_\sigma(\mathbf{r},t) \\ &\quad + \Delta\Theta(|z|-a)u_\sigma(\mathbf{r},t), \end{aligned} \tag{2.2}$$

where $\rho_\sigma = +1(-1)$ is related to the spin projection $\sigma = \uparrow(\downarrow)$, and $\Theta(z)$ stands for the Heaviside step function. The vector potential $\mathbf{A}(z,t)$ is related to the electric field by $\mathbf{A} = -c\mathbf{F}t$, where the electric field due to the voltage V is $\mathbf{F} = -\mathbf{e}_z(V/2a)\Theta(a-|z|)$. The chemical potential is denoted by μ; $e = +|e|$. Equal Fermi velocities in the F and S region are assumed. The magnetic scattering is neglected, since one can believe that in diluted magnetic alloys with a weak exchange energy the magnetic inhomogeneity is weak enough to result in a sufficiently small value of the magnetic scattering rate.[29]

We also assume that the two Ss are identical, and neglecting self-consistency, we approximate the spatial variation of the pair potential in the SFS junction by the step function $\Delta\Theta(|z|-a)$, where Δ is the bulk superconducting gap. The temperature dependence of Δ is given by $\Delta(T) = \Delta(0)\tanh(1.74\sqrt{T_c/T-1})$.[34]

Following KGN, we use an approximate solution of the BdGE, Eq. (2.2), in the form of a four-component spinor $\Psi(\mathbf{r},t) = [u_\uparrow(\mathbf{r},t), u_\downarrow(\mathbf{r},t), v_\uparrow(\mathbf{r},t), v_\downarrow(\mathbf{r},t)]^T$, valid under the condition

$$\frac{\hbar^2 k_{zf}^2}{2m} \gg |E \pm eV|, \tag{2.3}$$

where E is the energy eigenvalue for $V = 0$ and $k_{zf} = (k_f^2 - k_{||}^2)^{1/2}$ is the z component of the Fermi wave vector. Since the parallel component of the wave vector, $\mathbf{k}_\parallel = k_x\mathbf{e}_x + k_y\mathbf{e}_y$, is conserved due to translational invariance of the junction in directions perpendicular to the z axis, we can write $\Psi(\mathbf{r},t) = \psi(z,t)e^{i\mathbf{k}_\parallel\mathbf{r}}$, where $\psi(z,t) = [u_\uparrow(z,t), u_\downarrow(z,t), v_\uparrow(z,t), v_\downarrow(z,t)]^T$.

To calculate the current density we need to know the solutions of the time-dependent BdGEs in the ferromagnetic layer. Determination of unknown coefficients in these solutions requires matching at the boundaries $z = \pm a$ the wave functions in the F layer with the solutions of the BdGEs in superconducting layers. This is presented in the Appendix with the wave function in the F layer,

$$\psi_F^\pm(z,t,E_k) = \begin{pmatrix} u_{k\uparrow}^\pm(z,t) \\ u_{k\downarrow}^\pm(z,t) \\ v_{k\uparrow}^\pm(z,t) \\ v_{k\downarrow}^\pm(z,t) \end{pmatrix} = \sum_{n=-\infty}^{+\infty}\left[\begin{pmatrix}1\\0\\0\\0\end{pmatrix}u_{n\uparrow}^\pm(z,t,k) + \begin{pmatrix}0\\1\\0\\0\end{pmatrix}u_{n\downarrow}^\pm(z,t,k) + \begin{pmatrix}0\\0\\1\\0\end{pmatrix}v_{n\uparrow}^\pm(z,t,k) + \begin{pmatrix}0\\0\\0\\1\end{pmatrix}v_{n\downarrow}^\pm(z,t,k)\right], \tag{2.4}$$

where the superscript $+$ $(-)$ refers to positive (negative) z momentum.

Using the results from Appendix, we get the wave packets $u_{n\sigma}^\pm$ and $v_{n\sigma}^\pm$ related to the corresponding AR,[11]

$$u_{n\sigma}^+(z,t,k) = Ne^{-\frac{i}{\hbar}E_{2n\sigma}^+ t}e^{ik_{2n\sigma}^+ z}e^{i\varphi_+^\sigma}e^{-[((4n+1)a+z-v_{zf}t)\frac{\delta}{2\hbar v_{zf}}]^2}A_{2n}^+\left(E_k+\frac{eV}{2}+\rho_\sigma h\right), \tag{2.5}$$

$$u_{n\sigma}^-(z,t,k) = Ne^{-\frac{i}{\hbar}E_{2n\sigma}^- t}e^{-ik_{2n\sigma}^- z}e^{i\varphi_-^\sigma}e^{-[((4n+1)a-z-v_{zf}t)\frac{\delta}{2\hbar v_{zf}}]^2}A_{2n}^-\left(E_k-\frac{eV}{2}+\rho_\sigma h\right), \tag{2.6}$$

$$v^{+}_{n\sigma}(z,t,k) = Ne^{-\frac{i}{\hbar}E^{+}_{(2n+1)\sigma}t}e^{ik^{+}_{(2n+1)\sigma}z}e^{i\phi^{\sigma}_{+}}e^{-[((4n+3)a-z-v_{zf}t)\frac{\delta}{2\hbar v_{zf}}]^2}A^{+}_{2n+1}\left(E_k+\frac{eV}{2}-\rho_\sigma h\right), \tag{2.7}$$

$$v^{-}_{n\sigma}(z,t,k) = Ne^{-\frac{i}{\hbar}E^{-}_{(2n+1)\sigma}t}e^{-ik^{-}_{(2n+1)\sigma}z}e^{i\phi^{\sigma}_{-}}e^{-[((4n+3)a+z-v_{zf}t)\frac{\delta}{2\hbar v_{zf}}]^2}A^{-}_{2n+1}\left(E_k-\frac{eV}{2}-\rho_\sigma h\right), \tag{2.8}$$

with

$$E^{\pm}_{2n\sigma} = \pm 2neV \pm \frac{eV}{2} + eV\frac{z}{2a} + E_k + \rho_\sigma h, \tag{2.9}$$

$$E^{\pm}_{(2n+1)\sigma} = \pm(2n+1)eV \pm \frac{eV}{2} - eV\frac{z}{2a} + E_k - \rho_\sigma h, \tag{2.10}$$

$$k^{\pm}_{2n\sigma} = k_{zf} + (E^{\pm}_{2n\sigma} + \rho_\sigma h)\frac{1}{\hbar v_{zf}}, \tag{2.11}$$

$$k^{\pm}_{(2n+1)\sigma} = k_{zf} - \left(E^{\pm}_{(2n+1)\sigma} - \rho_\sigma h\right)\frac{1}{\hbar v_{zf}}. \tag{2.12}$$

In the presence of exchange energy in the F, $A^{\pm}_{2n}(E_k \pm \frac{eV}{2} + h)$, $A^{\pm}_{2n}(E_k \pm \frac{eV}{2} - h)$, $A^{\pm}_{2n+1}(E_k \pm \frac{eV}{2} + h)$, and $A^{\pm}_{2n+1}(E_k \pm \frac{eV}{2} - h)$, as defined by Eqs. (A19), (A20), (A11), and (A12), are the probability amplitudes that a quasiparticle at energy $E_k \pm h$ starts to move as an electron against (+) or opposite to (−) the field will reappear in the F region as an electron after $2n$ ARs and as a hole after $2n+1$ ARs, respectively.

According to Eqs. (2.5)–(2.12) the $E^{\pm}_{2n\sigma}$, $E^{\pm}_{(2n+1)\sigma}$, $k^{\pm}_{2n\sigma}$, and $k^{\pm}_{(2n+1)\sigma}$ are the instantaneous local energies and momenta of quasiparticle wave packets.[11,30] $\varphi^{\sigma}_{\pm}$ and $\phi^{\sigma}_{\pm}$ are irrelevant phase factors. The normalization factor N is determined by the probability P_N of finding a quasiparticle in the F layer where the electric field exists.[11]

III. CURRENT DENSITY

Using the gauge-invariant momentum operator $\mathbf{P} = [-i\hbar\nabla + e\mathbf{A}/c]$, and the relaxation-time approximation, one obtains the averaged current density in the F barrier,

$$\begin{aligned}\langle \mathbf{j}\rangle = -\frac{e}{4m}\hat{\sum_k}\{&f_0(E_k+h)(\langle u^{+*}_{k\uparrow}\mathbf{P}u^{+}_{k\uparrow}\rangle + \langle u^{-*}_{k\uparrow}\mathbf{P}u^{-}_{k\uparrow}\rangle) + f_0(E_k-h)(\langle u^{+*}_{k\downarrow}\mathbf{P}u^{+}_{k\downarrow}\rangle + \langle u^{-*}_{k\downarrow}\mathbf{P}u^{-}_{k\downarrow}\rangle)\\ &+(1-f_0(E_k+h))(\langle v^{+}_{k\uparrow}\mathbf{P}v^{+*}_{k\uparrow}\rangle + \langle v^{-}_{k\uparrow}\mathbf{P}v^{-*}_{k\uparrow}\rangle) + (1-f_0(E_k-h))(\langle v^{+}_{k\downarrow}\mathbf{P}v^{+*}_{k\downarrow}\rangle + \langle v^{-}_{k\downarrow}\mathbf{P}v^{-*}_{k\downarrow}\rangle)\},\end{aligned} \tag{3.1}$$

where f_0 is the Fermi distribution function. The caret over the summation sign means the sum over the complete set of positive- and negative-energy eigenstates E_k. The spatial and time integration in the averaged momentum densities,

$$\langle u^{\pm*}_{k\sigma}\mathbf{P}u^{\pm}_{k\sigma}\rangle = \frac{1}{2a}\frac{1}{t_c}\int_{-a}^{+a}dz\int_0^{\tau}dt e^{-t/T_S}u^{\pm*}_{k\sigma}(z,t)\mathbf{P}u^{\pm}_{k\sigma}(z,t), \tag{3.2}$$

$$\langle v^{\pm}_{k\sigma}\mathbf{P}v^{\pm*}_{k\sigma}\rangle = \frac{1}{2a}\frac{1}{t_c}\int_{-a}^{+a}dz\int_0^{\tau}dt e^{-t/T_S}v^{\pm}_{k\sigma}(z,t)\mathbf{P}v^{\pm*}_{k\sigma}(z,t), \tag{3.3}$$

are calculated in the same way as in Sec. III of Ref. 11, where τ is the time after which the quasiparticle has been accelerated to the edge of the pair potential well and left the F layer into one of the superconducting banks. It can be shown[11] that τ enters only in two added irrelevant functions that can be dropped out of the momentum densities, Eqs. (3.2) and (3.3). In this way it can be seen that the current density $\langle \mathbf{j}\rangle$, whose x and y components are 0, may be split into two terms:

$$\langle \mathbf{j}\rangle = \langle \mathbf{j}_N\rangle + \langle \mathbf{j}_{\mathrm{AR}}\rangle. \tag{3.4}$$

The term

$$\langle \mathbf{j}_N\rangle = -\mathbf{e}_z\frac{V}{R_N L_x L_y}, \tag{3.5}$$

where R_N is the normal resistance, corresponds to the ohmic current density, while the term $\langle \mathbf{j}_{\mathrm{AR}}\rangle$ is the current density due to AR,

$$\begin{aligned}\langle \mathbf{j}_{\mathrm{AR}}\rangle = -\mathbf{e}_z\frac{e}{2m}\frac{\hbar}{\Omega_N}\sum_k\sum_{n=1}^{\infty}P_N(E_k)e^{-\frac{2na}{l}}\Big\{&[(f_0(E_k+h)k_{e\uparrow}-(1-f_0(E_k+h))k_{h\downarrow})\\ &+(f_0(E_k-h)k_{e\uparrow}-(1-f_0(E_k-h))k_{h\downarrow})]\left[\left|A^{+}_n\left(E_k+\frac{1}{2}eV+h\right)\right|^2-\left|A^{-}_n\left(E_k-\frac{1}{2}eV+h\right)\right|^2\right]\end{aligned}$$

$$+[(f_0(E_k-h)k_{e\downarrow}-(1-f_0(E_k-h))k_{h\uparrow})+(f_0(E_k+h)k_{e\downarrow}-(1-f_0(E_k+h))k_{h\uparrow})]\left[\left|A_n^+\left(E_k+\frac{1}{2}eV-h\right)\right|^2-\left|A_n^-\left(E_k-\frac{1}{2}eV-h\right)\right|^2\right]\Bigg\}, \tag{3.6}$$

where

$$k_{e\sigma}=k_{zf}+\frac{E_k+\rho_\sigma h}{\hbar v_{zf}}, \tag{3.7}$$

$$k_{h\sigma}=k_{zf}-\frac{E_k-\rho_\sigma h}{\hbar v_{zf}}, \tag{3.8}$$

and $\Omega_N=2aL_xL_y$ is the volume of ferromagnetic layer. The terms proportional to the momentum changes in the electric field are omitted in Eq. (3.6) because they can be neglected for the same reason as in Ref. 11. The sum $\sum_k$, which is the sum over positive energies $E_k\geqslant 0$ only, can be transformed into an integral by introducing the DOS $g(E)$,

$$\sum_k\equiv\frac{1}{2}\int g(E)dE, \tag{3.9}$$

where the factor $1/2$ takes into account that only one z momentum direction is to be considered, whereas $g=(g_\uparrow+g_\downarrow)/2$. To calculate the current density, Eq. (3.6), we need to know g and P_N. The DOS is found from[13]

$$g_r(E)=\frac{L_xL_y}{\pi}\sum_r k_{zf,r}\left|\frac{dE}{dk_{zf}}\right|^{-1}_{k_{zf,r}}, \tag{3.10}$$

where $k_{zf,r}$ defines the value of k_{zf} for which $E_r=E$. The energy spectrum $E(k_{zf})$ consists of the spatially quantized bound states and the quasicontinuum scattering states. For spatially quantized Andreev bound states we calculate the spin-dependent DOS $g_{r,\sigma}$ from Eq. (3.10), with $E=E_\sigma$. The energies $E_\sigma<\Delta$ are the solutions of the transcendental equation (which can only be solved numerically)[35]

$$\cos\gamma_\sigma=\pm E_\sigma/\Delta, \tag{3.11}$$

where

$$\gamma_\sigma=\left(\frac{\phi}{2}\pm\frac{2ah}{\hbar v_{zf}}-\frac{2aE_\sigma}{\hbar v_{zf}}\right). \tag{3.12}$$

Here ϕ is the phase difference at the electrodes, $v_{zf}=v_f\cos\varphi$ and φ is the angle of the direction of the quasiparticle propagation with respect to the z axis perpendicular to the barrier. Note that for s-wave symmetry in the S, with the isotropic order parameter, the partial DOS (PDOS) for $\varphi=0$ coincides with the integral DOS, obtained by averaging the PDOS values for all φ over the Fermi surface.[32] Thus in the following we take $\varphi=0$.

For quasiparticles from quasicontinuum states, the energy spectrum is approximated by the continuous BCS spectrum of a homogeneous S:

$$E(k_{zf})=\left(\frac{\hbar^2}{2m}\left(k_f^2-k_{zf}^2\right)+\Delta^2\right)^{1/2}. \tag{3.13}$$

Then the density of quasicontinuum scattered states for $E>\Delta$ is[13]

$$g(E)=\frac{L_xL_y}{\pi^2}\frac{2m}{\hbar^2}k_f D\frac{E}{\sqrt{E^2-\Delta^2}}. \tag{3.14}$$

The probability $P_N(E)$ of finding quasiparticles with energy E in the F layer is given by Eq. (2.19) of Ref. 11,

$$P_N(E)=\frac{2a}{2a+2\lambda}, \tag{3.15}$$

with the penetration depth $\lambda=\frac{\hbar^2}{m}\frac{k_{zf}}{\sqrt{\Delta^2-E^2}}$ for $E<\Delta$, $\lambda<D-a$ and $\lambda=D-a$ otherwise. For quasiparticles from the scattering states, $E>\Delta$, $P_N(E)=2a/2D$.

When calculating the current density $\langle\mathbf{j}_{\mathrm{AR}}\rangle$ by integrating over the DOS, one has a finite integrand only in the range of nonvanishing multiple Andreev scattering probabilities $|A_n^\pm|^2$. Neglecting over-the-barrier reflections, these probabilities can be approximated by a step-function product,[11]

$$\left|A_n^\pm\left((E\pm h)\pm\tfrac{1}{2}eV\right)\right|^2\approx\Theta(\Delta\pm(E\pm h)+eV)\Theta(\Delta\mp(E\pm h)-neV). \tag{3.16}$$

In this way Eq. (3.6) becomes

$$\begin{aligned}\langle\mathbf{j}_{\mathrm{AR}}\rangle=-\mathbf{e}_z\frac{e}{2m}\frac{\hbar}{\Omega_N}\sum_{n=1}^{\infty}e^{-\frac{2na}{l}}\Bigg\{&\int_0^{E_1}dEg(E)[(f_0(E_k+h)k_{e\uparrow}-(1-f_0(E_k+h))k_{h\downarrow})+(f_0(E_k-h)k_{e\uparrow}-(1-f_0(E_k-h))k_{h\downarrow})]\\&-\int_{E_2'}^{E_2''}dEg(E)[(f_0(E_k+h)k_{e\uparrow}-(1-f_0(E_k+h))k_{h\downarrow})+(f_0(E_k-h)k_{e\uparrow}-(1-f_0(E_k-h))k_{h\downarrow})]\\&+\int_{E_3'}^{E_3''}dEg(E)[(f_0(E_k-h)k_{e\downarrow}-(1-f_0(E_k-h))k_{h\uparrow})+(f_0(E_k+h)k_{e\downarrow}-(1-f_0(E_k+h))k_{h\uparrow})]\\&-\int_{E_4'}^{E_4''}dEg(E)[(f_0(E_k-h)k_{e\downarrow}-(1-f_0(E_k-h))k_{h\uparrow})+(f_0(E_k+h)k_{e\downarrow}-(1-f_0(E_k+h))k_{h\uparrow})]\Bigg\},\end{aligned} \tag{3.17}$$

where

$$E_1 = \begin{cases} 0, & \Delta - neV - h \leqslant 0, \\ \Delta - neV - h & \text{otherwise;} \end{cases} \quad (3.18)$$

$$E_2^{'} = \begin{cases} 0, & neV - \Delta - h \leqslant 0, \\ neV - \Delta - h & \text{otherwise;} \end{cases} \quad (3.19)$$

$$E_2^{''} = \begin{cases} 0, & \Delta + eV - h \leqslant 0, \\ \Delta + eV - h & \text{otherwise;} \end{cases} \quad (3.20)$$

$$E_3^{'} = \begin{cases} 0, & -\Delta - eV + h \leqslant 0, \\ -\Delta - eV + h & \text{otherwise;} \end{cases} \quad (3.21)$$

$$E_3^{''} = \begin{cases} 0, & \Delta + h - neV \leqslant 0, \\ \Delta + h - neV & \text{otherwise;} \end{cases} \quad (3.22)$$

$$E_4^{'} = \begin{cases} 0, & neV - \Delta + h \leqslant 0, \\ neV - \Delta + h & \text{otherwise;} \end{cases} \quad (3.23)$$

$$E_4^{''} = \Delta + h + eV. \quad (3.24)$$

IV. RESULTS AND DISCUSSION

In the SFS case, the shape of CVCs depends on several parameters. Besides those important in the SNS case, such as the barrier thickness $d = 2a$, the mean free path l in the barrier, and the temperature T, of crucial importance here is the value of the exchange energy h in F. We discuss all these effects, but we would like to point out first that distinct structures of CVCs are found for h not to large, $h \lesssim \Delta$. A similar conclusion was found in a study[29] of phase-coherent transport in diffusive voltage-biased SFS plane junctions. For h equal to a few Δ, the effects of AR are still visible, in particular at low voltages, for small d and relatively large l.

In experiments with weakly ferromagnetic alloys in the barrier, the value of h is of the order of several (up to 10) Δ. However, one can expect that in the near-future it will be possible to prepare ferromagnetic alloys with a weaker exchange energy.[29]

Working with $l > d$ and $d \lesssim \xi_0$, we find that for h smaller than or of the order of Δ, CVCs can show several characteristic features. Similarly to the SNS case, CVCs can exhibit a rapid rise in the current at low voltages (the "foot" or "shoulder" of the characteristics) and arch-like structures with sometimes negative differential conductivity near the beginning of the curves. However, the presence and positions of irregularities in CVCs are strongly influenced by the value of the exchange energy h in the barrier.

In the following, we introduce reduced units: energies are reduced by $\Delta(T)$, $\tilde{h} = h/\Delta(T)$, $\tilde{V} = eV/\Delta(T)$, whereas $\tilde{d} = d/\xi_0$ and $\tilde{l} = l/\xi_0$. The total current, including the contributions of the ohmic current and of the AR current, $I = I_N + I_{AR} = L_x L_y(\langle j_N \rangle + \langle j_{AR} \rangle)$, is normalized by the temperature-dependent current $I_0 = 2\Delta(T)/eR_N$. In all examples we have chosen the parameters of the junction to correspond to the clean case (see below).

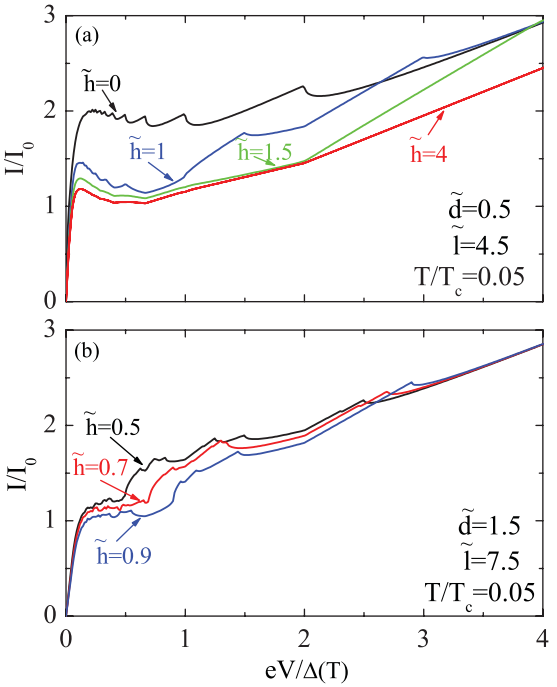

FIG. 2. (Color online) (a) Current-voltage characteristic $I(V)$ for $T/T_c = 0.05$, $l/\xi_0 = 4.5$, $d/\xi_0 = 0.5$, and four values of the exchange energy $h/\Delta(T)$: 0, 1, 1.5, and 4 (from top to bottom). (b) Current-voltage characteristic $I(V)$ for $T/T_c = 0.05$, $l/\xi_0 = 7.5$, $d/\xi_0 = 1.5$, and three values of the exchange energy $h/\Delta(T)$: 0.5, 0.7, and 0.9 (from top to bottom).

The effects of the exchange energy $\tilde{h}$ in the F on CVCs, shown in all figures, are illustrated, in particular, in Fig. 2. One can distinguish two types of effects.

(1) With increasing $\tilde{h}$, CVCs are shifted down in a large domain of voltages;

(2) For $\tilde{h} \lesssim 1$, we find that, in comparison with the SNS case,[11] there are new, $\tilde{h}$-induced structures in CVCs; and for $\tilde{h} \gg 1$, CVCs are monotonous and there are no additional structures.

The first effect is expected since, according to Upadhyay *et al.*[36] and de Jong and Beenaker,[37] for an FS contact, AR should be sensitive to polarization of the conduction electrons in the F. Not every electron with spin-up can find a spin-down electron with which to pair, and which then would be Andreev retroreflected from the F/S interface as a hole. The corresponding Cooper pair thus will not be able to form and enter into the S. This should reduce AR as $\tilde{h}$ increases, since the electron and the hole lose the correlation due to the exchange-energy-induced band splitting in F.[31]

As for the second effect, we note that in diffusive SFS junctions with nontransparent S/F interfaces, the appearance of additional h-dependent structures in CVCs (and in the conductance curves) found for intermediate values of Thouless energies, $\epsilon_{Th} \sim \Delta$, was explained by the change in the DOS in the presence of the exchange field.[29] In the present case, these structures, certainly influenced by the change in DOS and by the shift of energies $\tilde{E}_k \to \tilde{E}_k \pm \tilde{h}$, are primarily affected by the effects of $\tilde{h}$ on AR. The AR probabilities determine the limits of integrals contributing to $\langle \mathbf{j}_{AR} \rangle$, Eq. (3.17). When the range of one of the integrals in Eq. (3.17) shrinks to 0, there

is no contribution of AR at the corresponding voltage. From Eq. (3.17) it is easy to see that for the last three integrals this occurs at $\tilde{V}_n = 2/(n-1)$, i.e., at the same voltages as in the SNS case.[11] As for the first integral, its contribution to the current is practically zero, as can be seen from the numerical calculations.

For $\tilde{h}$-dependent structures, we find the following results.

(1) For $\tilde{h} \gtrsim 1$ [Fig. 2(a)], the nonlinearities of CVCs progressively disappear with increasing $\tilde{h}$. For comparison the curve for the SNS case, $\tilde{h} = 0$, is also shown.

(2) For $\tilde{h} < 1$ [Fig. 2(b)], the voltage range $\tilde{V} < \tilde{h}$ is the domain of many ARs. In the voltage range $\tilde{V} > \tilde{h}$ there are pronounced structures with one or two peaks between each two voltages $\tilde{V}_{n+1}$ and $\tilde{V}_n$. The results of our numerical calculations show that, similarly to the SNS case, for $\tilde{V} > \tilde{V}_n$ there are only $n-1$ or less ARs. For example, for $\tilde{V} > \tilde{V}_2 = 2$ there is only one harmonic, $n-1=1$, for $\tilde{V} > \tilde{V}_3 = 1$, $n-1=2$, etc. For $\tilde{V} > \tilde{V}_n$ the CVCs calculated with the corresponding small number of harmonics (a few n) coincide exactly with those obtained with $n = 100$ or more. In particular, there is always one peak for $\tilde{V} > 2$, absent in the SNS case. The range of voltage with several ARs, $\tilde{V} > \tilde{h}$, diminishes with increasing $\tilde{h}$, the number and the positions of peaks being $\tilde{h}$ dependent: when $\tilde{h}$ increases, the number of peaks decreases, while the distance between them changes. We find that the distance between the two highest voltage peaks is $2\tilde{h}$, the first three peaks being situated at $\tilde{V} = (2+\tilde{h})$, $\tilde{V} = (2-\tilde{h})$, and $\tilde{V} = (2+\tilde{h})/(n-1)$, respectively.

The influence of barrier thickness can be seen in Fig. 3. We note that for a relatively large $\tilde{l}$ and thin F barrier, there is a steep rise in CVCs at low voltages. The shape of the curves depend, first, on $\tilde{d}$, whereas the number of irregularities is determined by $\tilde{h}$. With increasing barrier thickness $\tilde{d}$, CVCs shift down, and the structures of CVCs progressively disappear, especially for large $\tilde{h}$. This is in accordance with the results of the theoretical study of plane SNS diffusive junctions by Cuevas *et al.*[38]

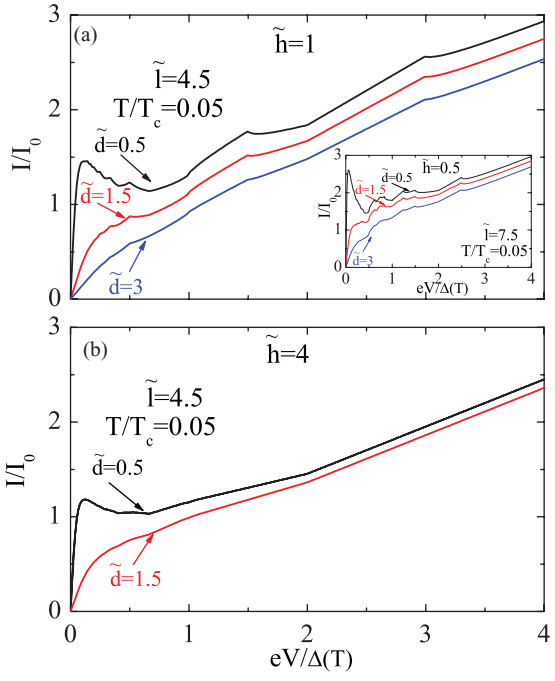

FIG. 3. (Color online) (a) Current-voltage characteristic $I(V)$ for $h/\Delta(T) = 1$, $l/\xi_0 = 4.5$, $T/T_c = 0.05$, and three values of the barrier thickness d/ξ_0: 0.5, 1.5, and 3 (from top to bottom). Inset: The same (a) for $h/\Delta(T) = 0.5$ and $l/\xi_0 = 7.5$. (b) Current-voltage characteristic $I(V)$ for $h/\Delta(T) = 4$, $l/\xi_0 = 4.5$, $T/T_c = 0.05$, and two values of the barrier thickness d/ξ_0: 0.5 (top) and 1.5 (bottom).

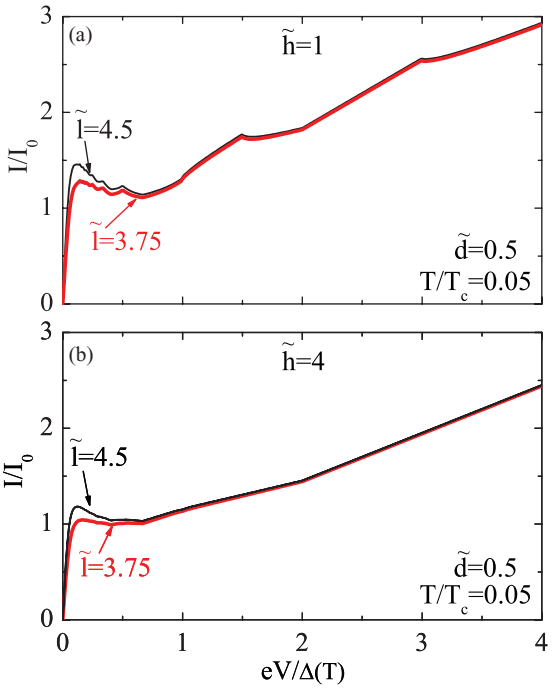

FIG. 4. (Color online) Current-voltage characteristic $I(V)$ for $T/T_c = 0.05$, $d/\xi_0 = 0.5$, and two values of the mean free path in the barrier l/ξ_0: 4.5 (top) and 3.75 (bottom). (a) $h/\Delta(T) = 1$. (b) $h/\Delta(T) = 4$.

The effect of the mean free path $\tilde{l}$ is presented in Fig. 4, where it is shown that with diminishing $\tilde{l}$, CVCs decrease at low voltages. For $\tilde{V} \gtrsim 1$ there is only a little difference between the CVCs for large but different mean free paths. Note that the junctions can be in the clean or dirty regime, according to the values of $\tilde{l}$ and $\tilde{h}$ for fixed $\tilde{d}$: for $\tilde{l} > \tilde{d}$, $\tilde{l} > (\pi/\tilde{h})(\Delta(0)/\Delta(T))$ this is the clean case, and for opposite inequalities, the dirty case.[21] The presented CVCs result from calculations with junction parameters chosen to correspond to the clean case.

With increasing temperature, CVCs also decrease (see Fig. 5). The physical reason is the same as in the SNS case. The number of thermally excited quasiparticles increases, and the AR contribution of quasiparticles with negative z momentum can cancel that due to quasiparticles with positive momentum [see Eq. (3.6)], which is the generalization of the KGN, Eq. (3.28) of Ref. 11. Again, more pronounced nonlinear structures are obtained for lower exchange energies $\tilde{h}$ and at lower temperatures.

Until now, considering the SNS case, we have relied on the results of KGN theory. However, it is worthwhile to comment briefly on a comparison of our results with those of the generalized theory of Gunsenheimer and Zaikin.[15]

(1) As in the SNS case,[11,15] we find that there is a current enhancement at low voltages, due to multiple ARs.

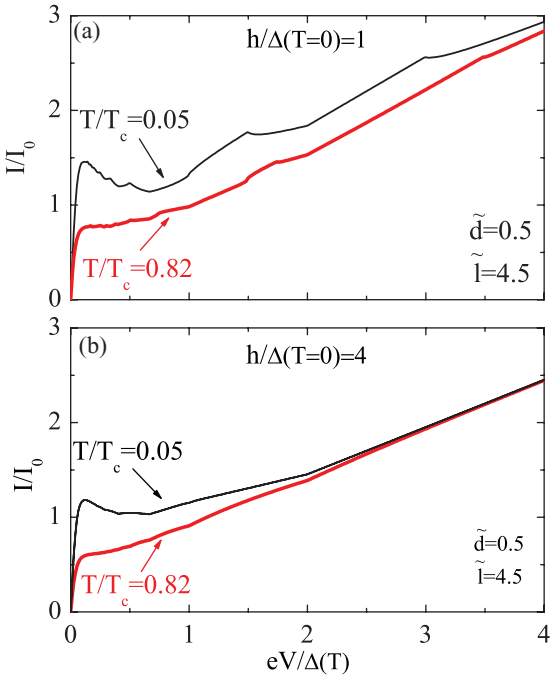

FIG. 5. (Color online) Current-voltage characteristic $I(V)$ for $d/\xi_0 = 0.5$, $l/\xi_0 = 4.5$, and two values of the temperature T/T_c: 0.05 (top) and 0.82 (bottom). (a) $h/\Delta(0) = 1$. (b) $h/\Delta(0) = 4$.

However, in the SFS case, the corresponding range of voltages is determined primarily by the value of the exchange energy h.

(2) Similarly to the SNS case,[11,15] characteristic voltages $V_n = \frac{\Delta/e}{n-1}$ play a role in determining the nonlinearities of CVCs. For SFS junctions and $eV/\Delta > h$ the peaks in CVCs occur between each two voltages eV_{n+1}/Δ and eV_n/Δ; see above.

(3) In Ref. 15 it was found that the amplitude of subgap peaks reaches a maximum at $k_BT \sim \Delta$, diminishing both at low and at high temperatures. In the present case, we find that the nonlinearities in CVCs disappear with increasing temperature, for the same reason as invoked in Ref. 11.

Finally, let us discuss briefly a comparison of our results with existing experimental data obtained in the dynamic regime. As stated above, even in SFS junctions with a weakly ferromagnetic barrier the exchange energy is $h \gtrsim \Delta$. In this case, we find that CVCs are always monotonous. For $h = 4\Delta$ CVCs calculated in the clean limit are similar to those obtained experimentally in diffusive junctions; see, e.g., Sellier *et al.*[20] for $d < \xi_0$ and Krasnov *et al.*[25] for $d > \xi_0$. For $h < \Delta$ there are still no experimental data.

V. CONCLUSION

In conclusion, we have presented a theory for CVCs of SFS weak links. The model operates for different barrier thicknesses d, the mean free path in the barrier $l > d$, and different temperatures $T < T_c$. Our main result is that rich structures in CVCs are obtained for a weak exchange energy, $h \lesssim \Delta$, for clean junctions. The model can be used for more general cases, but for arbitrary l a modification of the expression for the current would be necessary,[11] whereas the DOS could be calculated including the effect of impurity scattering. The calculation could also be generalized to the case of d-wave symmetry in superconducting electrodes. Both these tasks will be the subject of our future work.

In the present case, for a given exchange energy the shape of CVCs depends, first, on the barrier thickness. The presence and number of the nonlinear structures are determined by the exchange energy as well as the position of peaks: with increasing h the number of peaks diminishes, the distance between the two highest voltage peaks found for $h < \Delta$ increases, whereas for h of the order of a few Δ the peaks disappear completely. We believe that the predicted behavior could be measured in SFS systems realized on the basis of weak ferromagnetic alloys and that our results would trigger experimental activity on the fabrication of such alloys with $h \lesssim \Delta$.

Our work paves the way for the study of other transport properties in SFS systems, such as unusual Shapiro steps in 45° misoriented d-wave S/F/d-wave S junctions, where superharmonic current-phase relations have been predicted.[39]

ACKNOWLEDGMENT

The work was supported by the Serbian Ministry of Science, Project No. 171033.

APPENDIX

In the F layer, $-a < z < a$, the solution of BdGE is

$$\psi_F(z,t) = C_1^+ \begin{pmatrix}1\\0\\0\\0\end{pmatrix} u_\uparrow^+ + C_1^- \begin{pmatrix}1\\0\\0\\0\end{pmatrix} u_\uparrow^- + C_2^+ \begin{pmatrix}0\\1\\0\\0\end{pmatrix} u_\downarrow^+ + C_2^- \begin{pmatrix}0\\1\\0\\0\end{pmatrix} u_\downarrow^- + C_3^+ \begin{pmatrix}0\\0\\1\\0\end{pmatrix} v_\uparrow^+ + C_3^- \begin{pmatrix}0\\0\\1\\0\end{pmatrix} v_\uparrow^- + C_4^+ \begin{pmatrix}0\\0\\0\\1\end{pmatrix} v_\downarrow^+ + C_4^- \begin{pmatrix}0\\0\\0\\1\end{pmatrix} v_\downarrow^-, \tag{A1}$$

with

$$u_\uparrow^\pm = e^{-\frac{i}{\hbar}(E+eV\frac{z}{2a})t} e^{\pm i q_1^+ z}, \tag{A2}$$

$$u_\downarrow^\pm = e^{-\frac{i}{\hbar}(E+eV\frac{z}{2a})t} e^{\pm i q_1^- z}, \tag{A3}$$

$$v_\uparrow^\pm = e^{-\frac{i}{\hbar}(E-eV\frac{z}{2a})t} e^{\pm i q_2^- z}, \tag{A4}$$

$$v_\downarrow^\pm = e^{-\frac{i}{\hbar}(E-eV\frac{z}{2a})t} e^{\pm i q_2^+ z} \tag{A5}$$

and

$$q_1^\pm = k_{zf} + \frac{1}{\hbar v_{zf}}\left(E + eV\frac{z}{2a} \pm h\right), \tag{A6}$$

$$q_2^\pm = k_{zf} - \frac{1}{\hbar v_{zf}}\left(E - eV\frac{z}{2a} \pm h\right), \tag{A7}$$

where $v_{zf} = \hbar k_{zf}/m$ is the z component of the Fermi velocity.

In superconducting banks, $|z| > a$, we have

$$\psi_S(z,t) = e^{-\frac{i}{\hbar}Et}\left\{\left[D_1^+\begin{pmatrix}1\\0\\0\\\nu\end{pmatrix} + F_1^+\begin{pmatrix}0\\1\\\nu\\0\end{pmatrix}\right]e^{ik^+z}\Theta(z-a) + \left[D_1^-\begin{pmatrix}1\\0\\0\\\nu\end{pmatrix} + F_1^-\begin{pmatrix}0\\1\\\nu\\0\end{pmatrix}\right]e^{-ik^+z}\Theta(-z-a)\right.$$
$$\left. + \left[D_2^+\begin{pmatrix}1\\0\\0\\\nu^{-1}\end{pmatrix} + F_2^+\begin{pmatrix}0\\1\\\nu^{-1}\\0\end{pmatrix}\right]e^{ik^-z}\Theta(-z-a) + \left[D_2^-\begin{pmatrix}1\\0\\0\\\nu^{-1}\end{pmatrix} + F_2^-\begin{pmatrix}0\\1\\\nu^{-1}\\0\end{pmatrix}\right]e^{-ik^-z}\Theta(z-a)\right\}, \quad \text{(A8)}$$

with

$$k^\pm = \left[k_{zf}^2 \pm i\frac{2m}{\hbar^2}(\Delta^2 - E^2)^{1/2}\right]^{1/2} \approx k_{zf} \pm i\frac{m}{\hbar^2}\frac{(\Delta^2-E^2)^{1/2}}{k_{zf}} \quad \text{for} \quad E < \Delta, \quad \text{(A9)}$$

$$k^\pm = \left[k_{zf}^2 \pm \frac{2m}{\hbar^2}(E^2 - \Delta^2)^{1/2}\right]^{1/2} \approx k_{zf} \pm \frac{m}{\hbar^2}\frac{(E^2-\Delta^2)^{1/2}}{k_{zf}} \quad \text{for} \quad E > \Delta, \quad \text{(A10)}$$

$$\nu = \frac{E - i(\Delta^2 - E^2)^{1/2}}{\Delta} \quad \text{for} \quad E < \Delta, \quad \text{(A11)}$$

$$\nu = \frac{E - (E^2 - \Delta^2)^{1/2}}{\Delta} \quad \text{for} \quad E > \Delta. \quad \text{(A12)}$$

Electrons and holes with the same direction of z momentum are coupled together by Andreev scattering and are decoupled from electrons and holes with the opposite direction of z momentum. As a consequence, in the same way as in Ref. 11, wave functions (A1) and (A8) split into the two independent solutions which refer to positive and negative z momentum. The most general solution of the time-dependent BdGE is the sum of all positive- and negative-energy solutions:

$$\psi_S^\pm(z,t) = \int_{-\infty}^{+\infty} dE\,\psi_S^\pm(E,z,t), \quad \text{(A13)}$$

$$\psi_F^\pm(z,t) = \int_{-\infty}^{+\infty} dE\,\psi_F^\pm(E,z,t). \quad \text{(A14)}$$

Neglecting the ordinary reflection processes for sufficiently large k_{zf}, we have to match only the wave amplitudes, Eqs. (A1) and (A8), at the phase boundaries $z = \pm a$.[30] This results in the following recursion equations for the coefficients of the F-layer wave functions:

$$C_1^\pm(E \pm n2eV) = C_1^\pm(E)e^{i(4n(E+h)\pm 4n^2eV)\frac{a}{\hbar v_{zf}}}A_{2n}^\pm(E), \quad \text{(A15)}$$

$$C_4^\pm(E \pm n2eV) = C_1^\pm(E \mp eV)e^{i((4n+2)(E+h)\pm 4n^2eV\mp eV)\frac{a}{\hbar v_{zf}}}A_{2n+1}^\pm(E), \quad \text{(A16)}$$

$$C_2^\pm(E \pm n2eV) = C_2^\pm(E)e^{i(4n(E-h)\pm 4n^2eV)\frac{a}{\hbar v_{zf}}}A_{2n}^\pm(E), \quad \text{(A17)}$$

$$C_3^\pm(E \pm n2eV) = C_2^\pm(E \mp eV)e^{i((4n+2)(E-h)\pm 4n^2eV\mp eV)\frac{a}{\hbar v_{zf}}}A_{2n+1}^\pm(E). \quad \text{(A18)}$$

Here the multiple AR probability amplitudes are

$$A_{2n}^\pm(E) = \prod_{l=1}^{2n}\nu(E \pm leV \mp eV/2), \quad \text{(A19)}$$

$$A_{2n+1}^\pm(E) = \prod_{l=1}^{2n+1}\nu(E \pm leV \mp eV/2), \quad \text{(A20)}$$

and

$$A_0^\pm(E) = 1, \quad \text{(A21)}$$

while $|\nu(\varepsilon)|^2$ is the probability that an AR occurs at energy ε in the phase boundary of a semi-infinite superconducting bank.

Because of the recursion relation, Eqs. (A15)–(A18), the coefficients $C_4^\pm$ and $C_3^\pm$ are completely determined by the coefficients $C_1^\pm$ and $C_2^\pm$, respectively, which in turn can be chosen freely only within an energy interval of width $2eV$. We build wave packets with a Gaussian momentum distribution by choosing[11,30]

$$C_1^\pm(E) = \frac{N}{\sqrt{\pi\delta^2}}e^{[(E-\gamma_{k\uparrow})/\delta]^2}e^{i\frac{E}{\hbar v_{zf}}a}, \quad \text{(A22)}$$

$$C_2^\pm(E) = \frac{N}{\sqrt{\pi\delta^2}}e^{[(E-\gamma_{k\downarrow})/\delta]^2}e^{i\frac{E}{\hbar v_{zf}}a}, \quad \text{(A23)}$$

with

$$n_k 2eV \leqslant \gamma_{k\sigma} \leqslant (n_k+1)2eV, \quad \text{(A24)}$$

where n_k is an integer. The inequality $\delta^2 < (2eV)^2$ ensures that the amplitudes of $C_1^\pm(E)$ and $C_2^\pm(E)$ are low outside the interval (A24), while $\gamma_{k\sigma}$ is the wave-packet energy in the center of the F layer before the first AR occurs. We choose the same initial energy distribution C_1^+ and C_1^-, Eq. (A22) [and C_2^+ and C_2^-, Eq. (A23), for wave packets with opposite momenta], since equilibrium states with positive and negative z momenta are degenerate. We can split the integral of Eq. (A14) into energy intervals of width $2eV$ and relate these intervals to the initial one defined by Eq. (A24), with the help of the recursion equations (A15)–(A18).

In this way, generalizing the procedure for the SNS case,[11] we can write the wave function in the F layer as

$$\psi_F^{\pm}(z,t,E_k) = \begin{pmatrix} u_{k\uparrow}^{\pm}(z,t) \\ u_{k\downarrow}^{\pm}(z,t) \\ v_{k\uparrow}^{\pm}(z,t) \\ v_{k\downarrow}^{\pm}(z,t) \end{pmatrix} = \sum_{n=-\infty}^{+\infty} \left[\begin{pmatrix} 1 \\ 0 \\ 0 \\ 0 \end{pmatrix} u_{n\uparrow}^{\pm}(z,t,k) + \begin{pmatrix} 0 \\ 1 \\ 0 \\ 0 \end{pmatrix} u_{n\downarrow}^{\pm}(z,t,k) + \begin{pmatrix} 0 \\ 0 \\ 1 \\ 0 \end{pmatrix} v_{n\uparrow}^{\pm}(z,t,k) + \begin{pmatrix} 0 \\ 0 \\ 0 \\ 1 \end{pmatrix} v_{n\downarrow}^{\pm}(z,t,k) \right] \tag{A25}$$

with

$$u_{n\uparrow}^{\pm}(z,t,k) = \int_{n_k 2eV}^{(n_k+1)2eV} dE C_1^{\pm}(E \pm n2eV) u_{\uparrow}^{\pm}(E \pm n2eV), \tag{A26}$$

$$u_{n\downarrow}^{\pm}(z,t,k) = \int_{n_k 2eV}^{(n_k+1)2eV} dE C_2^{\pm}(E \pm n2eV) u_{\downarrow}^{\pm}(E \pm n2eV), \tag{A27}$$

$$v_{n\uparrow}^{\pm}(z,t,k) = \int_{n_k 2eV \pm eV}^{(n_k+1)2eV \pm eV} dE C_3^{\pm}(E \pm n2eV) v_{\uparrow}^{\pm}(E \pm n2eV), \tag{A28}$$

$$v_{n\downarrow}^{\pm}(z,t,k) = \int_{n_k 2eV \pm eV}^{(n_k+1)2eV \pm eV} dE C_4^{\pm}(E \pm n2eV) v_{\downarrow}^{\pm}(E \pm n2eV). \tag{A29}$$

We evaluate previous integrals with the help of Eqs. (A2)–(A5), relations (A15)–(A21), and Gaussians (A22) and (A23). With the definition

$$\gamma_{k\sigma} = E_k \pm \frac{eV}{2} + \rho_\sigma h, \tag{A30}$$

this results in Eqs. (2.5)–(2.12).

---

*Corresponding author: zikicradomir@yahoo.com

[1] A. A. Golubov, M. Yu. Kupriyanov, and E. Ilichev, Rev. Mod. Phys. **76**, 411 (2004).

[2] A. I. Buzdin, Rev. Mod. Phys. **77**, 935 (2005).

[3] F. S. Bergeret, A. F. Volkov, and K. B. Efetov, Rev. Mod. Phys. **77**, 1321 (2005).

[4] A. F. Andreev, Zh. Eksp. Teor. Fiz. **49**, 655 (1965); Sov. Phys. JETP **22**, 455 (1966).

[5] I. O. Kulik, Zh. Eksp. Teor. Fiz. **57**, 1745 (1969).

[6] I. O. Kulik, Sov. Phys. JETP **30**, 944 (1970).

[7] J. Bardeen and J. L. Johnson, Phys. Rev. B **5**, 72 (1972).

[8] A. Furusaki and M. Tsukada, Phys. Rev. B **43**, 10164 (1991).

[9] S. K. Yip, Phys. Rev. B **58**, 5803 (1998).

[10] H. Sellier, C. Baraduc, F. Lefloch, and R. Calemczuk, Phys. Rev. B **68**, 054531 (2003).

[11] R. Kümmel, U. Gunsenheimer, and R. Nicolsky, Phys. Rev. B **42**, 3992 (1990).

[12] M. Octavio, W. J. Skocpol, and M. Tinkham, Phys. Rev. B **17**, 159 (1978); H. C. Yang, C. H. Nien, H. H. Sung, and C. H. Chen, J. Low Temp. Phys. **45**, 243 (1989).

[13] D. M. Gokhfeld, Supercond. Sci. Technol. **20**, 62 (2007).

[14] V. N. Gubankov, V. P. Koshelets, and G. A. Ovsyannikov, Fiz. Nizk. Temp. **7**, 560 (1981).

[15] U. Gunsenheimer and A. D. Zaikin, Phys. Rev. B **50**, 6317 (1994).

[16] A. Martín-Rodero, A. Levy Yeyati, and J. C. Cuevas, Physica C **352**, 67 (2001).

[17] V. V. Ryazanov, V. A. Oboznov, A. Y. Rusanov, A. V. Veretennikov, A. A. Golubov, and J. Aarts, Phys. Rev. Lett. **86**, 2427 (2001); V. V. Ryazanov, V. A. Oboznov, A. V. Veretennikov, and A. Y. Rusanov, Phys. Rev. B **65**, 020501(R) (2001).

[18] T. Kontos, M. Aprili, J. Lesueur, F. Genêt, B. Stephanidis, and R. Boursier, Phys. Rev. Lett. **89**, 137007 (2002).

[19] Y. Blum, A. Tsukernik, M. Karpovski, and A. Palevski, Phys. Rev. Lett. **89**, 187004 (2002).

[20] H. Sellier, C. Baraduc, F. Lefloch, and R. Calemczuk, Phys. Rev. Lett. **92**, 257005 (2004).

[21] J. W. A. Robinson, S. Piano, G. Burnell, C. Bell, and M. G. Blamire, Phys. Rev. B **76**, 094522 (2007).

[22] A. A. Bannykh, J. Pfeiffer, V. S. Stolyarov, I. E. Batov, V. V. Ryazanov, and M. Weides, Phys. Rev. B **79**, 054501 (2009).

[23] J. Pfeiffer, M. Kemmler, D. Koelle, R. Kleiner, E. Goldobin, M. Weides, A. K. Feofanov, J. Lisenfeld, and A. V. Ustinov, Phys. Rev. B **77**, 214506 (2008).

[24] F. Born, M. Siegel, E. K. Hollmann, H. Braak, A. A. Golubov, D. Yu. Gusakova, and M. Yu. Kupriyanov, Phys. Rev. B **74**, 140501(R) (2006).

[25] V. M. Krasnov, O. Ericsson, S. Intiso, P. Delsing, V. A. Oboznov, A. S. Prokofiev, and V. V. Ryazanov, Physica C **418**, 16 (2005).

[26] M. Weides, M. Kemmler, H. Kohlstedt, R. Waser, D. Koelle, R. Kleiner, and E. Goldobin, Phys. Rev. Lett. **97**, 247001 (2006); M. Weides, Ph.D. thesis, Forschungszentrums Jülich, 2007.

[27] A. S. Vasenko, S. Kawabata, A. A. Golubov, M. Yu. Kupriyanov, C. Lacroix, F. S. Bergeret, and F. W. J. Hekking, Phys. Rev. B **84**, 024524 (2011).

[28] M. Anderson, J. C. Cuevas, and M. Fogelstrom, Physica C **367**, 117 (2002); I. V. Bobkova, Phys. Rev. B **73**, 012506 (2006).

[29] I. V. Bobkova and A. M. Bobkov, Phys. Rev. B **74**, 220504(R) (2006).

[30] R. Kümmel and W. Senftinger, Z. Phys. B **59**, 275 (1985).

[31] O. Vávra, Š. Gaži, I. Vávra, J. Dérer, and E. Kováčova, Physica C **404**, 395 (2004).

[32] R. Zikic, L. Dobrosavljević-Grujić, and Z. Radović, Phys. Rev. B **59**, 14644 (1999).

[33]Z. Pajović, M. Božović, Z. Radović, J. Cayssol, and A. I. Buzdin, Phys. Rev. B **74**, 184509 (2006).
[34]B. Muhlschlegel, Z. Phys. **155**, 313 (1959).
[35]L. Dobrosavljević-Grujić, R. Zikic, and Z. Radović, Physica C **331**, 254 (2000).
[36]S. K. Upadhyay, A. Palanisami, R. N. Louie, and R. A. Buhrman, Phys. Rev. Lett. **81**, 3247 (1998).
[37]M. J. M. de Jong and C. W. J. Beeenakker, Phys. Rev. Lett. **74**, 1657 (1995).
[38]J. C. Cuevas, J. Hammer, J. Kopu, J. K. Viljas, and M. Eschrig, Phys. Rev. B **73**, 184505 (2006).
[39]R. Zikic and L. Dobrosavljević-Grujić, Phys. Rev. B **75**, 100502(R) (2007).